Biochemistry

pubs.acs.org/biochemistry Article

Fungally Derived Isoquinoline Demonstrates Inducer-Specific Tau Aggregation Inhibition

David J. Ingham,* Bryce R. Blankenfeld, Shibin Chacko, Chamani Perera, Berl R. Oakley, and Truman Christopher Gamblin*

Cite This: *Biochemistry* 2021, 60, 1658−1669 Read Online

ACCESS | Metrics & More | Article Recommendations | Supporting Information

ABSTRACT: The microtubule-associated protein tau promotes the stabilization of the axonal cytoskeleton in neurons. In several neurodegenerative diseases, such as Alzheimer's disease, tau has been found to dissociate from microtubules, leading to the formation of pathological aggregates that display an amyloid fibril-like structure. Recent structural studies have shown that the tau filaments isolated from different neurodegenerative disorders have structurally distinct fibril cores that are specific to the disease. These "strains" of tau fibrils appear to propagate between neurons in a prion-like fashion that maintains their initial template structure. In addition, the strains isolated from diseased tissue appear to have structures that are different from those made by the most commonly used *in vitro* modeling inducer molecule, heparin. The structural differences among strains in different diseases and *in vitro*-induced tau fibrils may contribute to recent failures in clinical trials of compounds designed to target tau pathology. This study identifies an isoquinoline compound (ANTC-15) isolated from the fungus *Aspergillus nidulans* that can both inhibit filaments induced by arachidonic acid (ARA) and disassemble preformed ARA fibrils. When compared to a tau aggregation inhibitor currently in clinical trials (LMTX, LMTM, or TRx0237), ANTC-15 and LMTX were found to have opposing inducer-specific activities against ARA and heparin *in vitro*-induced tau filaments. These findings may help explain the disappointing results in translating potent preclinical inhibitor candidates to successful clinical treatments.

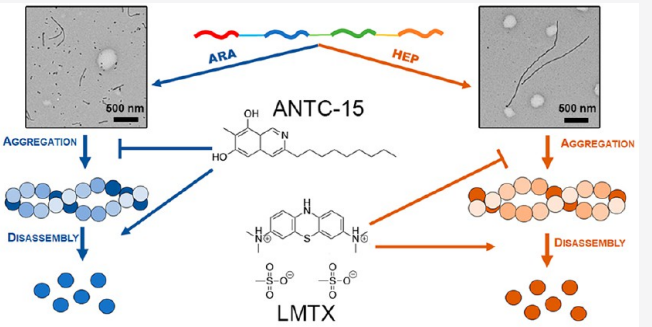

Aggregation of the microtubule-associated protein tau (MAPT, UniProtKB P10636) is a histopathological hallmark of multiple neurodegenerative diseases such as Alzheimer's disease (AD) and Alzheimer's disease-related dementias (ADRDs), including progressive supranuclear palsy (PSP), Pick's disease (PD), corticobasal degeneration (CBD), chronic traumatic encephalopathy (CTE), and frontotemporal dementias with Parkinsonism linked to chromosome 17 (FTDP-17). AD and ADRDs have huge impacts on the economy and healthcare in the United States with an estimated annual cost of more than $305 billion and with 5.8 million Americans diagnosed with AD or ADRDs.[1] Tau pathology has been linked to neuronal cell death, and its progression correlates extremely well with the advancement and severity of dementia.[2] To make matters worse, to date there are no FDA-approved therapeutics that prevent or slow the development of tau pathology.

Blocking or reversing tau aggregation is considered to be a viable therapeutic approach for the treatment of AD and ADRDs for the following reasons. Tau aggregation correlates with cellular dysfunction and neuronal death; there is no known normal biological function of tau aggregates, and extensive approaches targeting other pathological structures such as β-amyloid senile plaques have been unsuccessful.[3,4] There have therefore been multiple studies aimed at identifying small-molecule tau aggregation inhibitors (TAIs).[5] TAIs have traditionally been identified by screening large libraries of hundreds of thousands of small molecules against tau aggregates.[6] Due to the large amount of tau aggregate that is required to conduct these screens, it is impractical to use authentic tau filaments isolated from diseased tissue. Rather, it has been necessary to use recombinant tau that has been induced to form filaments *in vitro*.

The most common inducers employed for studying tau aggregation have been polyanionic molecules such as the glycosaminoglycan heparin, polyphosphate, and RNA; planar aromatic dyes such as Congo red and thiazine red; free fatty acids such as arachidonic acid and docosahexaenoic acid; and anionic detergents such as alkyl sulfate.[7] These compounds have been used primarily because the tau filaments induced in

Received: February 12, 2021
Revised: May 10, 2021
Published: May 19, 2021

https://doi.org/10.1021/acs.biochem.1c00111
Biochemistry 2021, 60, 1658−1669

their presence have gross morphological similarities to filaments isolated from diseased tissue. They have increased levels of β-strand formation like disease filaments; many of them bind to dyes such as thioflavin S in a manner similar to that of disease filaments, and antibodies that recognize aggregated tau in disease also interact with many of the *in vitro*-assembled filaments. Compounds based on a phenothiazine core structure, such as LMTX (leucomethylthionine, LMTM, or TRx0237), a compound that has had limited success in phase III clinical trials,[8] were identified primarily on the basis of their inhibition of heparin-induced tau aggregates.[9]

Emerging evidence has revealed that tau aggregates from disease do not all have identical structures;[10] rather, they form unique and distinct "strains" with different seeding capacities and three-dimensional structures.[11−13] This evidence strongly suggests that tau pathology between AD and other ADRDs is much more heterogeneous than previously thought.[11,12,14] The structural variability in aggregated tau conformations has important implications in the identification of effective TAIs.

Recently, multiple studies have shown the structure of heparin-induced filaments differs from those identified in diseased tissue.[15,16] As yet, there have not been any published high-resolution structures of arachidonic acid-induced tau filaments. As is the case with filament structures identified from diseased tissue, it is likely that different aggregation inducer molecules may result in heterogeneous filament structures. On the basis of comparisons of filament length distributions, polymerization kinetics, and polymerization conditions, it is highly likely that the core fibril folds formed by these inducers are different.[17]

We have previously identified secondary metabolites isolated from the fungus *Aspergillus nidulans* that are effective at inhibiting and disassembling arachidonic acid- and heparin-induced tau aggregates *in vitro*.[18,19] The most effective of these previously studied compounds was an azaphilone compound, Aza-9 {5-bromo-3-[(*S*,1*E*,3*E*)-3,5-dimethylhepta-1,3-dien-1-yl]-7-methyl-6,8-dioxo-7,8-dihydro-6*H*-isochromen-7-yl acetate}. Aza-9 was able to inhibit and disassemble tau aggregates induced by both heparin and arachidonic acid. However, Aza-9 also appeared to have high levels of nonspecific interactions with tubulin, as evidenced by tubulin polymerization studies,[19] suggesting the possibility that it has somewhat promiscuous activity toward proteins in general.

In this study, we show how a different fungal secondary metabolite with an isoquinoline structure, ANTC-15 (7-methyl-3-nonylisoquinoline-6,8-diol[20]), can act as a narrow spectrum TAI *in vitro*. We chose to study ANTC-15 because it is a naturally occurring compound that is structurally similar to other known tau aggregation inhibitors (for example, 4-piperazine isoquinoline derivatives[21]) and shares some structural similarities with the aforementioned Aza-9. We found that ANTC-15 both inhibits arachidonic acid (ARA)-induced aggregation and disassembles ARA PFFs with a potency greater than that of Aza-9 and could be a good candidate for further development because even though it has a cLogP above the range of most CNS penetrant drugs, the compound has not yet been modified in any way to increase its efficacy through structure−activity relationship studies. This is an initial examination of the properties of ANTC-15 before any efforts to increase its potency and drug-like characteristics. We compared the activities of ANTC-15 and LMTX against arachidonic acid- and heparin-induced tau filaments and studied their effects on tubulin polymerization. We have found that ANTC-15 inhibits the assembly of, and promotes the disassembly of, arachidonic acid-induced filaments but not heparin-induced filaments. LMTX, on the contrary, inhibits the assembly of heparin-induced filaments but is not effective against arachidonic acid-induced filaments. These results strongly suggest that heparin and ARA induce different polymorphs and ANTC-15 and LMTX have different activities against these polymorphs.

Together, these findings support the hypothesis that tau aggregation inhibitors of different classes may have inducer-specific mechanisms of action. Understanding how these different molecules interact with tau will be an important step in developing tau aggregation inhibitors that can target disease relevant strains.

MATERIALS AND METHODS

Chemicals and Reagents. Full length 2N4R tau (HT40, 441 amino acids) was expressed in *Escherichia coli* and purified, as previously described, by Ni-His Tag affinity purification and size exclusion chromatography.[22] As shown by King et al., the polyhistidine tag does not influence tau aggregation and therefore was not removed.[23] The tau protein concentration was quantified using a Pierce BCA protein assay kit (23225) purchased from Thermo Fisher Scientific. The tau was confirmed to be ∼95% pure by sodium dodecyl sulfate−polyacrylamide gel electrophoresis (data not shown). Individual aliquots of 50 μL were prepared and stored at −80 °C to avoid protein degradation. Arachidonic acid (90010) was purchased from Cayman Chemical (Ann Arbor, MI). Heparin sodium salt (H4784) with an average molecular weight of 17000−19000 Da was purchased from Millipore Sigma (St. Louis, MO). TRx0237 mesylate salt (LMTX) (CAS Registry No. 1236208-20-0) was purchased from BOC Sciences (Shirley, NY). ANTC-15 (7-methyl-3-nonylisoquinoline-6,8-diol) was discovered as a compound produced by overexpression of a nonreducing polyketide synthase (ANID_03386.1 = AN3386) in *A. nidulans*.[20] Additional quantities of ANTC-15 were synthesized by the University of Kansas synthetic chemical biology core facility. The structure of the synthesized compound was confirmed using ^{1}H NMR (500 MHz, DMSO-d_6), ^{13}C NMR (126 MHz, DMSO), and high-resolution mass spectrometry (HRMS). A schematic diagram and description of the synthesis can be found in Figure S1. TOC1 and TNT1 capture antibodies were a kind gift from N. Kanaan (Michigan State University, East Lansing, MI). The primary detection antibody was an anti-tau polyclonal rabbit antibody (A002401-2) purchased from Agilent (Santa Clara, CA). A goat anti-rabbit IgG (H+L) antibody with an HRP conjugate (1706515, Bio-Rad, Hercules, CA) was used as a secondary detection antibody.

Inhibition of Tau Aggregation. Inhibition assays of arachidonic acid-induced filaments were performed as previously described.[19] Two microliters of various concentrations of test compounds dissolved in DMSO were added to 190.5 μL of polymerization buffer (PB) in 1.7 mL microcentrifuge tubes to give a final compound concentration range of 0.8−200 μM. The final DMSO concentration was 1%. PB final concentrations were 100 mM NaCl, 5 mM DTT, 10 mM HEPES (pH 7.64), 0.1 mM EDTA, and 2 μM 2N4R tau. These mixtures of the compound and monomeric tau were incubated for 20 min at room temperature before the addition of 7.5 μL of 2 mM ARA dissolved in 100% ethanol (final volume of 200 μL, final ARA concentration of 75 μM).

https://doi.org/10.1021/acs.biochem.1c00111
Biochemistry 2021, 60, 1658−1669

Reactions were carried out overnight (20 h) at 25 °C. A no-compound polymer control containing 1% DMSO and 75 μM arachidonic acid and a no-compound monomer control of 1% DMSO and 0 μM arachidonic acid were used as positive and negative controls, respectively. Inhibition assays of heparin-induced filaments were carried out similarly but with the following modifications. The final NaCl concentration was 25 mM with a final concentration of 0.5 μM heparin dissolved in ddH_2O; no ethanol was added to any of the heparin reaction mixtures. Incubation was completed at 37 °C for 48 h.

Disassembly of Preformed Tau Filaments. Disassembly reactions were completed by setting up reactions in PB as described above prior to adding inhibitor compounds dissolved in DMSO. The reactions were given time for tau to completely polymerize (6 h for arachidonic acid-induced reactions and 48 h for heparin-induced reactions) before adding the inhibitor compound dissolved in DMSO to give a final compound concentration range of 0.8−400 μM (final DMSO concentration of 1%) in a 1.7 mL microcentrifuge tube. The reaction mixtures were then left to incubate for 24 h at 25 °C for arachidonic acid-induced filaments and 37 °C for heparin-induced filaments.

Sandwich ELISA. Following inhibition and disassembly reaction mixture incubations, samples were analyzed using a modified sandwich ELISA based on conditions previously described by Combs et al.[24] Briefly, a Corning 3590 EIA/RIA 96-well microplate was coated with 100 μL/well of capture antibody [either TOC1 (2 ng/μL) or TNT1 (1 ng/μL)], sealed, and incubated with gentle agitation overnight at 4 °C. Capture antibodies were diluted in BSB capture buffer [100 mM boric acid, 25 mM sodium tetraborate, 75 mM NaCl, and 250 μM thimerosal (pH 8.56)]. The plate was then washed twice with 300 μL of BSB wash buffer [100 mM boric acid, 25 mM sodium tetraborate, 75 mM NaCl, 250 μM thimerosal, 60 mM BSA, and 0.1% Tween 20 (pH 8.56)] per well. Each well was then blocked with 300 μL of 5% nonfat dry milk (NFDM) dissolved in BSB wash buffer, sealed, and incubated at room temperature for 1.5 h with gentle agitation. Inhibition or disassembly reaction samples were diluted in 5% NFDM BSB wash buffer to a concentration of 100 nM for the TOC1 capture antibody and 25 nM for TNT1. To provide an internal standard curve, dilution series of no-compound polymer and monomer controls were added to the plate in ranges of 3.125−400 nM for TOC1 and 3.125−75 nM for TNT. In our hands, the EC_{50} values of the polymerized tau affinity curve were found to be 105 and 28 nM for TOC1 and TNT1, respectively (see Figure S2 for antibody binding affinity curves). Samples were added to a volume of 100 μL/well. Plates were sealed and incubated at room temperature for 1.5 h with gentle agitation. Plates were then washed twice using BSB wash buffer. Next, 100 μL of polyclonal rabbit detection antibody per well diluted to a concentration of 50 ng/mL in 5% NFDM BSB wash buffer was added. Plates were sealed and incubated at room temperature for 1.5 h with gentle agitation. Plates were washed twice using BSB wash buffer before the addition of 100 μL of the goat anti-rabbit IgG secondary detection antibody per well diluted 1:5000 in 5% NFDM BSB wash buffer. The plate was sealed and incubated at room temperature with gentle agitation for 1.5 h. Plates were then washed thrice using BSB wash buffer before the addition of 50 μL of tetramethylbenzidine (TMB) substrate per well. The plates were then covered and incubated with gentle agitation at room temperature for 20 min before the addition of 50 μL of a 3.6% H_2SO_4 stop solution. Readings were taken at an absorbance of 450 nm using a Varian Cary 50 UV−vis spectrophotometer with a Varian Cary microplate reader. Raw data readings were zeroed against the no-compound monomeric control and then converted to percent light absorbance and normalized using the internal no-compound polymer control. Half-maximal inhibitory concentration (IC_{50}) and the half-maximal disassembly concentration (DC_{50}) values were calculated by fitting the data to a log(inhibitor) versus response−variable slope, nonlinear regression curve using Graphpad Prism 8.0. Curves were fit using the following variation of the 4PL equation where Top and Bottom refer to the upper and lower plateaus of the response curve, respectively.

$$Y = \text{Bottom} + (\text{Top} - \text{Bottom})(1 + 10^{\log \text{IC}_{50} - X} \times \text{Hill slope}) \quad (1)$$

Statistical analyses were completed using a one-way ANOVA multiple-comparison Tukey's test to compare values at a screening concentration of 200 μM and the no-compound control. Statistical significance was defined as $^{*}p \leq 0.05$, $^{**}p \leq 0.01$, and $^{***}p \leq 0.001$. A full summary of p values for all ARA-induced filament screening experiments can be found in Table S1, and all HEP-induced filament screening experiments in Table S2.

Transmission Electron Microscopy. Inhibition and disassembly samples were diluted 1:10 in polymerization buffer and fixed with 2% glutaraldehyde for 5 min at room temperature. The samples were then affixed to a 300-mesh carbon Formvar-coated copper grid, purchased from Electron Microscopy Sciences (Hatfield, PA), by floating the grid on a 10 μL droplet of sample for 1 min. The grid was then blotted on filter paper and washed on a droplet of ddH_2O before being blotted and stained by floating the grid on a droplet of 2% uranyl acetate as previously described.[25] The grids were imaged using a JEOL JEM 1400 transmission electron microscope fitted with a LaB_6 electron source (Electron Microscopy Research Lab, University of Kansas Medical Center). Five random images per grid were taken at a 5000× magnification. Images were analyzed using Image Pro Plus 6.0 software by measuring the number, length, area, and perimeter of >25 nm filaments. Under our experimental conditions, it is very difficult to reliably identify <25 nm filaments; therefore, the assay is limited to tau filaments and >25 nm oligomers. IC_{50} and DC_{50} values were determined by fitting the data to a log(inhibitor) versus response−variable slope nonlinear regression curve in Graphpad Prism 8.0 (see eq 1).

Tubulin Polymerization. Assays were completed in triplicate using tubulin polymerization assay kits (BK006P) purchased from Cytoskeleton Inc. (Denver, CO). Following the manufacturer's protocol for screening proteins for effects on tubulin polymerization activity, 0.5 μM tau was added using a multichannel pipet to a final concentration of 2 mg/mL tubulin protein with or without 40 μM ANTC-15 or LMTX diluted in DMSO. Tubulin polymerization was monitored at 340 nm using a Varian Cary UV−vis spectrophotometer with a Varian Cary microplate reader at 37 °C. Readings were taken every 60 s for 61 min. Data were fitted to the Finke−Watzky polymerization equation shown below and analyzed using a paired t test in Graphpad Prism 8.0.

https://doi.org/10.1021/acs.biochem.1c00111
Biochemistry 2021, 60, 1658−1669

$$[B]_t = [A]_0 - \frac{\frac{k_1}{k_2} + [A]_0}{1 + \frac{k_1}{k_2[A]_0}\exp(k_1 + k_2[A]_0)t} \quad (2)$$

where $[B]_t$ is the amount of tubulin polymerization at time t, k_1 is the nucleation rate, and k_2 is the elongation rate (reported k_1 and k_2 values can be found in Figure S3).

Acoustic Shearing of Heparin Filaments. No-compound 1% DMSO heparin-induced fibrils were formed as described above. Samples at volumes of 130 μL were transferred to Covaris microtube-130 AFA fiber preslit snapcap tubes (PN 500514). Samples were then sheared for 0, 30, 180, and 450 s using a Covaris ME220 focused ultrasonicator (Covaris Inc., Woburn, MA) at 20 °C on settings of 50 W peak power, 20% duty factor, and 200 cycles per burst. Using right-angle laser light, scattering samples were analyzed for their ability to scatter light as previously described.[26] Briefly, samples were transferred to a 5 mm × 5 mm optical glass cuvette (Starna Cells, Atascadero, CA) in the light path of a 532 nm wavelength 12 mW solid-state laser operating at 7.6 mW (B&W Tek Inc., Newark, DE), and images were captured using a Sony XC-ST270 digital camera with an aperture of f.s. 5.6. Images were analyzed using Adobe Photo Shop 2021 by taking histogram readings of the pixel intensity across the scattered light path. Following the sandwich ELISA protocol described above, samples were analyzed for their affinity for TOC1 and TNT1 capture antibodies as well as being imaged by TEM as described above.

RESULTS

In previous studies of secondary metabolites isolated from the fungus *A. nidulans*, we have identified multiple compounds that can both inhibit and disassemble tau filaments induced by arachidonic acid.[18,19] We have since identified a new class of fungal secondary metabolites that may act as tau aggregation inhibitors. The isoquinoline ANTC-15 (Figure 1A) was studied for its ability to inhibit and disassemble tau filaments *in vitro*. As an external benchmark, we wanted to compare the inhibitory activity of ANTC-15 to that of a known and extensively studied tau aggregation inhibitor, LMTX (Figure 1B). LMTX has been shown to inhibit and disassemble tau aggregates in both *in vitro* and *in vivo* models. In phase III clinical trials, it has shown limited success in the treatment of mild to moderate Alzheimer's disease.[8,27]

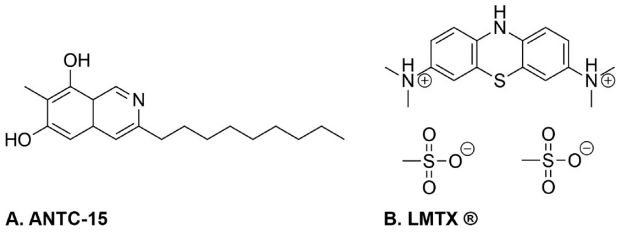

Figure 1. (A) Chemical structure of the isoquinoline ANTC-15 (7-methyl-3-nonylisoquinoline-6,8-diol). (B) Chemical structure of the phenothiazine LMTX (TRx0237, leuco-methylthionine mesylate salt).

Assembly Inhibition Assays. Typical tau aggregation inhibitor screening studies utilize high-throughput methods, such as thioflavin T and thioflavin S fluorescence. During studies of both of these compounds, we found that they interfered with thioflavin fluorescence at our initial screening concentration of 200 μM (Figure S4). We also found that both compounds scattered light in aqueous solutions, and we were therefore unable to use the standard right-angle laser light scattering aggregation assay (Figure S4). We therefore used a quantitative sandwich ELISA technique to determine the ability of ANTC-15 and LMTX to inhibit *in vitro* ARA-induced tau filament formation at an initial concentration of 200 μM (Figure 2A,B). The sandwich ELISA utilizes a polyclonal rabbit total tau detection antibody (A0024) and two monoclonal toxic-conformation-sensitive capture antibodies (TOC1 and TNT1) that have a high affinity for toxic tau species that are enriched during aggregation[24] with a linear dependence on the total amount of aggregates (Figure S2). The tau oligomeric complex (TOC1) antibody recognizes toxic tau oligomers that are induced by arachidonic acid and heparin, as well as pathological tau from Alzheimer's disease (AD) and chronic traumatic encephalopathy (CTE) brain tissue.[28−30] The tau N-terminal (TNT1) antibody recognizes the phosphatase-activating domain (PAD) of the N-terminus of tau, an epitope that is present in early stage tau aggregation generated *in vitro* and found in both AD and CTE brain tissue.[29,31]

In these assays, ANTC-15 almost completely inhibited the formation of both TOC1 and TNT1 reactive tau species that were induced by ARA (Figure 2A,B). In contrast, LMTX had no significant effect on the formation of TNT1 reactive species and caused a significant increase in the amount of TOC1 reactive species (Figure 2A,B). Transmission electron microscopy (TEM) was used to visualize the effect of these compounds over a range of concentrations (3−200 μM). Representative TEM micrographs show the effects of ANTC-15 (Figure 2E−H) and LMTX (Figure 2I−L) on ARA filament formation. Quantification of both the average number of filaments per image and the total filament length present on the TEM micrographs treated with 200 μM ANTC-15 confirmed that ANTC-15 significantly decreased the number and total length of tau filaments induced by ARA. LMTX at 200 μM, however, caused an increase in the length and numbers of filaments (Figure S5).

LMTX was first identified as a potent inhibitor of heparin-induced filaments.[9] We therefore compared the ability of LMTX and ANTC-15 to inhibit heparin induction of tau aggregation (Figure 3). There was a significant decrease in the levels of TOC1 and TNT1 reactive species in the presence of 200 μM LMTX; however, no significant difference was observed in the presence of 200 μM ANTC-15. Quantification of the average number of filaments per image and total filament length based on TEM micrographs confirmed the finding from the ELISA experiments that LMTX significantly inhibited the number and total length of heparin-induced filaments (Figure S5). Representative TEM micrographs (Figure 3E−H) show the effects of ANTC-15 and LMTX (Figure 3I−L) on heparin-induced filament formation.

Disassembly Assays. In disease, tau pathology is thought to develop long before symptom onset.[32] Therefore, to identify compounds that act as TAIs, it is also useful to determine if these molecules can disassemble preformed fibrils (PFFs). In addition, due to the structural stability of amyloid folds, compounds that are able to disassemble PFFs are unlikely to inhibit tau aggregation by interfering with the inducer mechanism. To evaluate the abilities of ANTC-15 and LMTX to disassemble PFFs, we added each compound after the filaments had fully polymerized, incubated the PFFs with

https://doi.org/10.1021/acs.biochem.1c00111
Biochemistry 2021, 60, 1658−1669

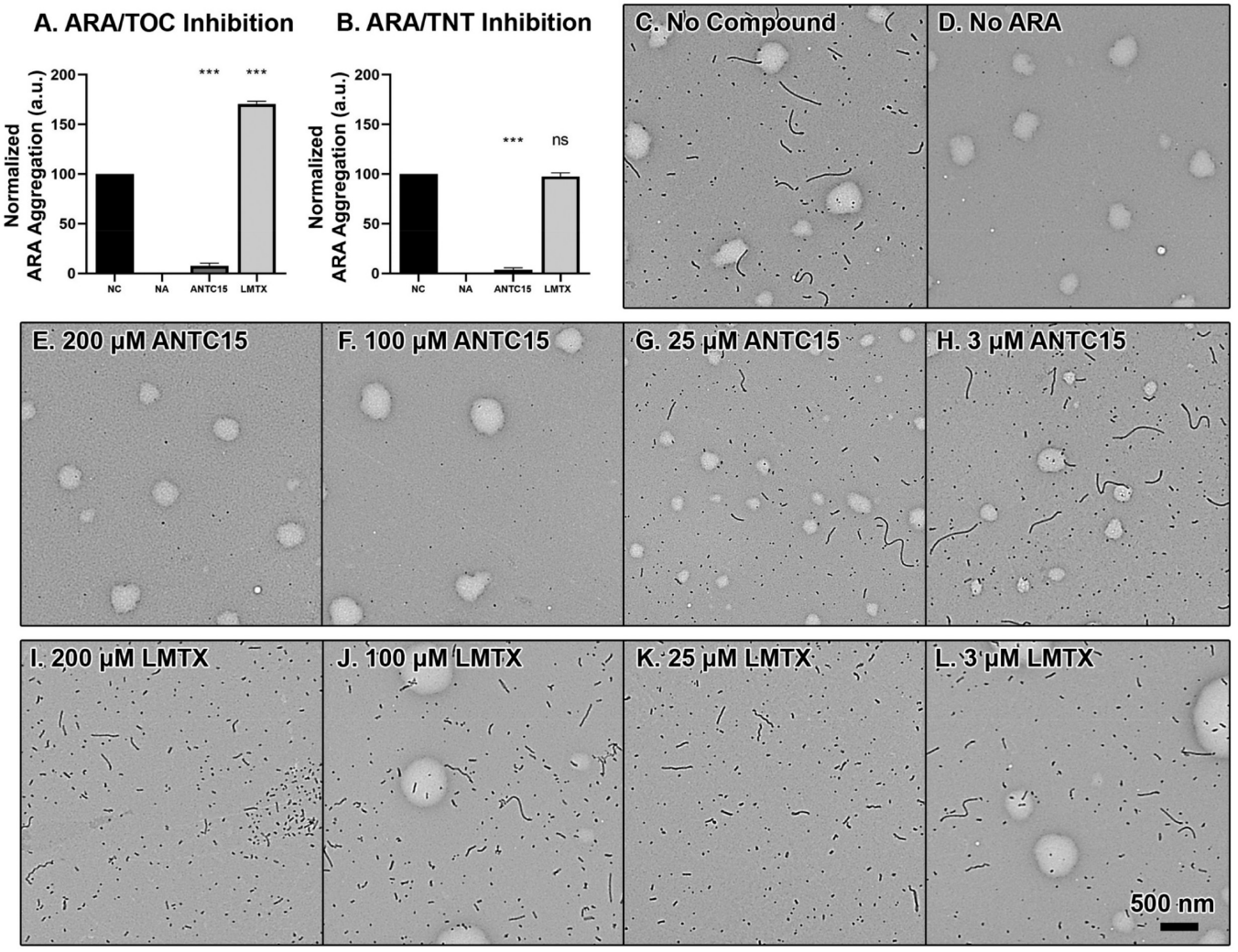

Figure 2. Initial inhibition assay of 200 μM ANTC-15 and LMTX against ARA-induced tau filaments. Sandwich ELISA using the TOC1 capture antibody and TNT1 capture antibody (A and B, respectively) normalized against the 1% DMSO no-compound control (no compound = 100). Samples were compared to the no-compound control using a Tukey's multiple-comparison test (p values of all comparisons can be found in Table S1): *$p \leq 0.05$, **$p \leq 0.01$, and ***$p \leq 0.001$. ns denotes no significant difference. Representative transmission electron micrographs at 5000× magnification of (C) the no-compound control, (D) the no-ARA monomer control, (E−H) ANTC-15, and (I−L) LMTX at concentrations of 200, 100, 25, and 3 μM (from left to right, respectively). The scale bar in panel L represents 500 nm for all images.

compound for 24 h, and then determined the amount of remaining aggregates by sELISA.

When ARA-induced PFFs were treated with 200 μM ANTC-15, there was a significant decrease in the levels of TOC1 and TNT1 reactive species (Figure 4A,B). There was approximately a 50% reduction in the level of TOC1 reactive species and a 40% reduction in the level of TNT1 reactive species. The addition of LMTX to ARA PFFs caused an increase in the level of TOC1 reactive species and had no effect on the level of TNT1 reactive species (Figure 4A,B), which is consistent with results from ARA aggregation induction trials (compare to Figure 2).

We also compared the activity of ANTC-15 and LMTX to disassemble heparin PFFs. There was no significant change in heparin-induced TOC1 and TNT1 reactive species with 200 μM ANTC-15 (Figure 4C,D). There were significant increases in the levels of TOC1 species in samples treated with 200 μM LMTX (Figure 4C); however, changes in the levels of TNT1 reactive species were not significantly different from that of the no-compound control when analyzed using a Tukey's multiple-comparison test (Figure 4 D). We were interested to see if the increase in the levels of TOC1 and TNT1 species observed in the presence of LMTX could be caused by the change in filament length distributions. Therefore, we used quantitative TEM to measure the changes in filament length distribution in samples treated with 200 μM LMTX. Compared to the no-compound control, an increase in the number of small filaments (25−50 nm) was observed with 200 μM LMTX (Figure S6).

Dose Dependence Studies. Due to ANTC-15's ability to inhibit and disassemble ARA-induced filaments at high concentrations, we sought to measure the relative efficacy of ANTC-15 by determining the values of IC_{50} and DC_{50} (Figure 5). ANTC-15 concentrations ranged from 3 to 400 μM, and experiments were completed in triplicate to establish an IC_{50} and a DC_{50} for each of the two antibodies that recognize toxic species of tau (TOC1 and TNT1) and by average number of filaments per image and total length of filaments as measured by TEM. Similar IC_{50} values were obtained by a sandwich ELISA for TOC1 and TNT1 tau species for ANTC-15 (35 and

https://doi.org/10.1021/acs.biochem.1c00111
Biochemistry 2021, 60, 1658−1669

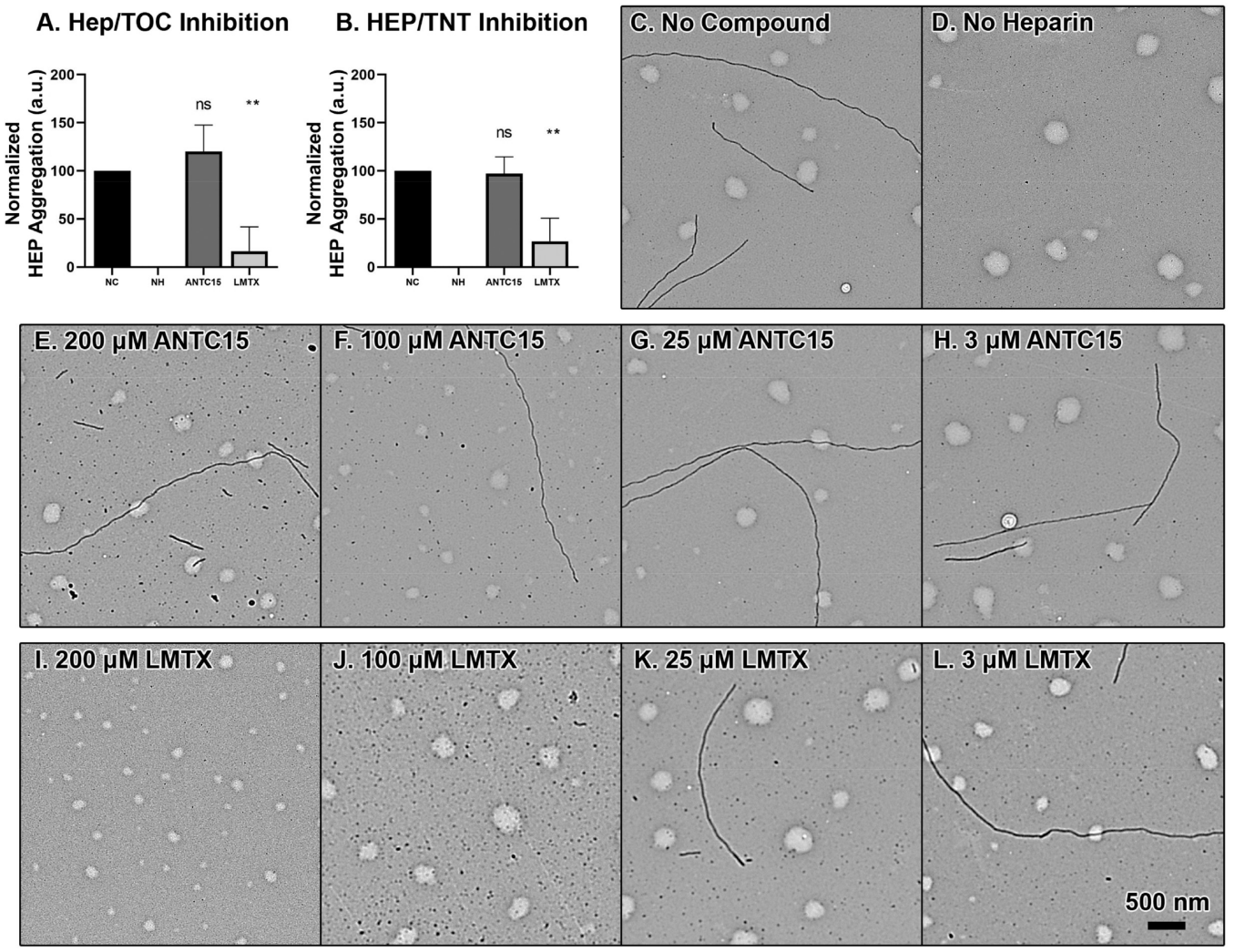

Figure 3. (A and B) Initial inhibition assay of 200 μM compound of ANTC-15 and LMTX against heparin (Hep)-induced tau filaments. Sandwich ELISA using the TOC1 capture antibody and TNT1 capture antibody (A and B, respectively) normalized against the 1% DMSO no-compound control (no compound = 100). Samples were compared to no-compound controls using a Tukey's multiple-comparison test (p values of all comparisons can be found in Table S1): *$p \leq 0.05$, **$p \leq 0.01$, and ***$p \leq 0.001$. ns denotes no significant difference. Representative transmission electron micrographs at 5000× magnification of (C) the no-compound control, (D) the no-heparin monomer control, (E−H) ANTC-15, and (I−L) LMTX at concentrations of 200, 100, 25, and 3 μM (from left to right, respectively). The scale bar in panel L represents 500 nm for all images.

47 μM, respectively). These values were in general agreement with IC_{50} values obtained by quantitative EM for the average number of filaments per image (33 μM) and the total filament length (25 μM) (Figure 5A,C,E). As determined by both a sandwich ELISA and EM, complete inhibition of ARA-induced aggregation occurred at approximately 100 μM.

Disassembly was assessed by quantitation of the TOC1 and TNT1 species remaining after incubation of ARA PFFs. At the highest concentration tested, ANTC-15 decreases the amount of PFF approximately 50% and 40%, respectively (Figure 5B). We cannot accurately determine the value of DC_{50} by a sELISA because, by definition, there cannot be a half-maximal concentration for disassembly if the amount of disassembly does not reach 100%. However, the sELISA results with TOC1 indicate that there is an estimated 50% reduction in PFF at an approximate compound concentration of 200 μM. Our analysis of the average number of filaments remaining after treatment of ARA PFFs with ANTC-15 using TEM revealed a decrease of approximately 90% in the average number of filaments at the highest ANTC-15 concentrations used (Figure 5D) and a decrease in the total filament length of approximately 80% (Figure 5F). Again, we are not able to accurately determine an absolute value for the DC_{50} as determined by TEM, but a rough estimation of the data suggests that there is a 50% reduction in the average number of PFFs at 200 μM and a 50% reduction in the total mass of ARA PFFs at 250 μM.

Analogous experiments using heparin-induced filaments to identify a dose-dependent response to LMTX were also completed (see Figure S7). However, the data from these experiments could not be used to calculate an IC_{50} and a DC_{50} for the following reasons. (1) LMTX appears to form many small tau oligomers that are reactive to both TOC1 and TNT1 antibodies and can be detected by TEM. Other groups have shown that this is the case with the closely related compound methylene blue with a reported IC_{50} value of 1.9 μM.[33] (2) The previously reported IC_{50} values of LMTX inhibition of tau filament formation in a cell free environment have been shown to be much lower than the IC_{50} based on cell free tau−tau binding assays (analogous to the sandwich ELISA used in this study).[34] Therefore, LMTX appears to interact with tau

https://doi.org/10.1021/acs.biochem.1c00111
Biochemistry 2021, 60, 1658−1669

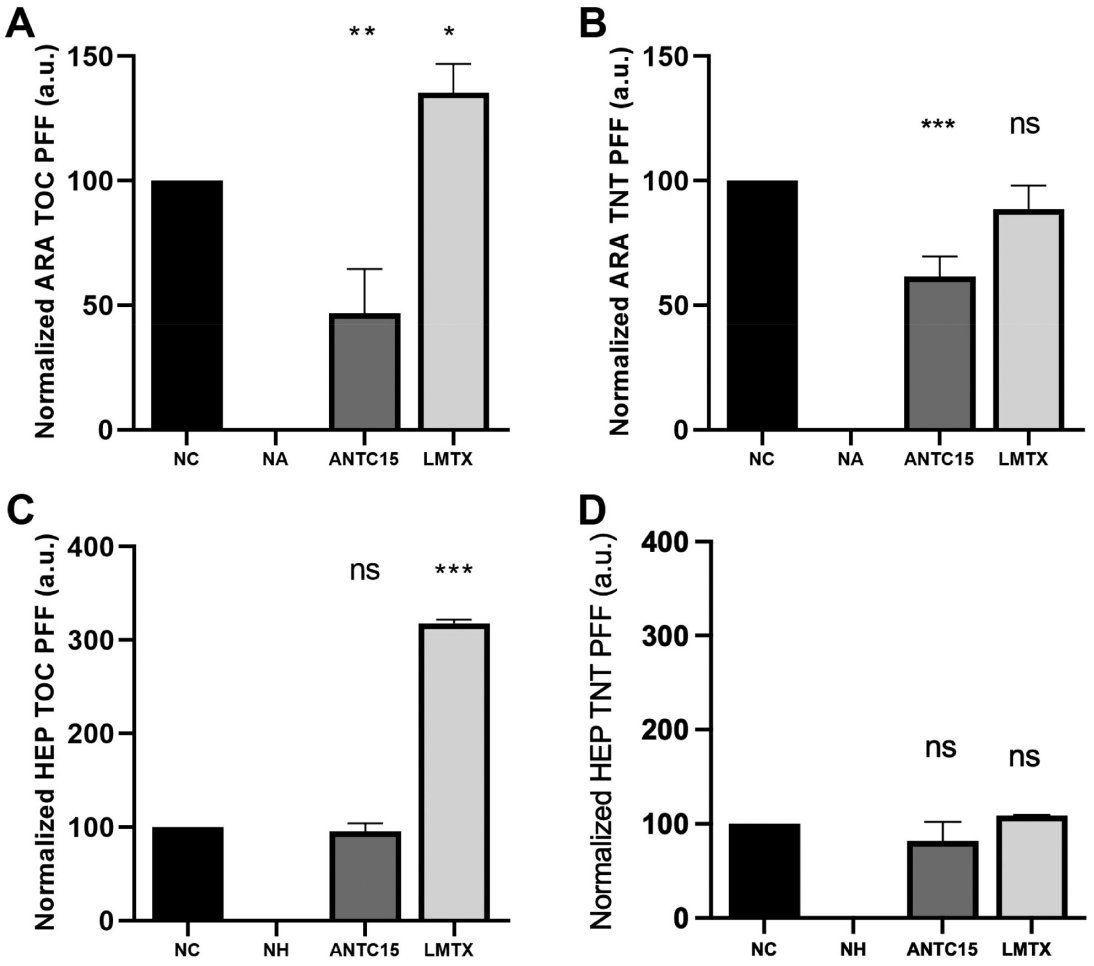

Figure 4. Disassembly assay of 200 μM ANTC-15 and LMTX against (A and B) ARA-induced tau filaments and (C and D) heparin-induced tau filaments. Sandwich ELISA using the TOC1 capture antibody (left) and TNT1 capture antibody (right) normalized against the 1% DMSO no-compound control (no compound = 100). Samples were compared to the no-compound control using a Tukey's multiple-comparison test (p values of all comparisons can be found in Table S2): *$p \leq 0.05$, **$p \leq 0.01$, and ***$p \leq 0.001$. ns denotes no significant difference.

through two different mechanisms: one that breaks down larger filaments into small oligomers within a low micromolar concentration range and one that blocks tau−tau binding in a high micromolar concentration range. (3) Because heparin-induced filaments are much longer than those induced by ARA, it is difficult to reliably measure subtle changes in total filament length and the number of filaments to be able to calculate IC_{50} and DC_{50} values. (4) The differences in how LMTX and other closely related molecules interact with heparin-induced tau filaments and cell-based tau aggregation assays have been extensively studied by other groups and therefore were considered to be outside the scope of this study.[33,34]

Tubulin Polymerization. An important feature of any potential TAI should be that it does not inhibit the normal functions of tau, due to the large potential for side effects through a toxic loss of tau function. We therefore compared the microtubule stabilization properties of tau with and without ANTC-15 and LMTX (Figure 6). The probability that the differences occurred by chance is 78% for ANTC-15 (p = 0.78) and 9% for LMTX (p = 0.09), which are both higher than the widely accepted 5% threshold for significance (p = 0.05). Similarly, neither ANTC-15 nor LMTX caused a significant change in the nucleation rate (k_1) in comparison with the tubulin-with-tau control, although the p values once again suggest the effect of ANTC-15 (0.7) is weaker than that of LMTX (0.13). However, the analysis did show a significant difference between the tubulin-with-tau elongation rate (k_2) and that of the samples with LMTX, but not with ANTC-15 (p values of 0.021 and 0.24, respectively). A summary table of tubulin polymerization assay p values is provided in Figure S3, along with graphs of the maximum polymerization, elongation rate (k_1), elongation rate (k_2), and data for tubulin only with and without ANTC-15 and LMTX.

DISCUSSION

There has been a recent realization of the need for treatments for Alzheimer's disease and Alzheimer's disease-related dementias that directly reduce the level of pathological accumulation of aggregated tau. There have been efforts to reduce the level of expression of tau, to reduce the number of post-translational modifications of tau, to increase the rate of clearance of abnormal tau, to repair the functional loss of tau by stabilizing microtubules, to reduce the prion-like spread of tau, and to inhibit or reverse the aggregation of tau.[35]

Techniques such as PET imaging, cognitive diagnostic tests, and analysis of post mortem tissue have shown that the underlying pathology of tau aggregation can occur in neurons many years, or even decades, prior to symptom onset and disease diagnosis.[36] Therefore, it is important to be able to

https://doi.org/10.1021/acs.biochem.1c00111
Biochemistry 2021, 60, 1658−1669

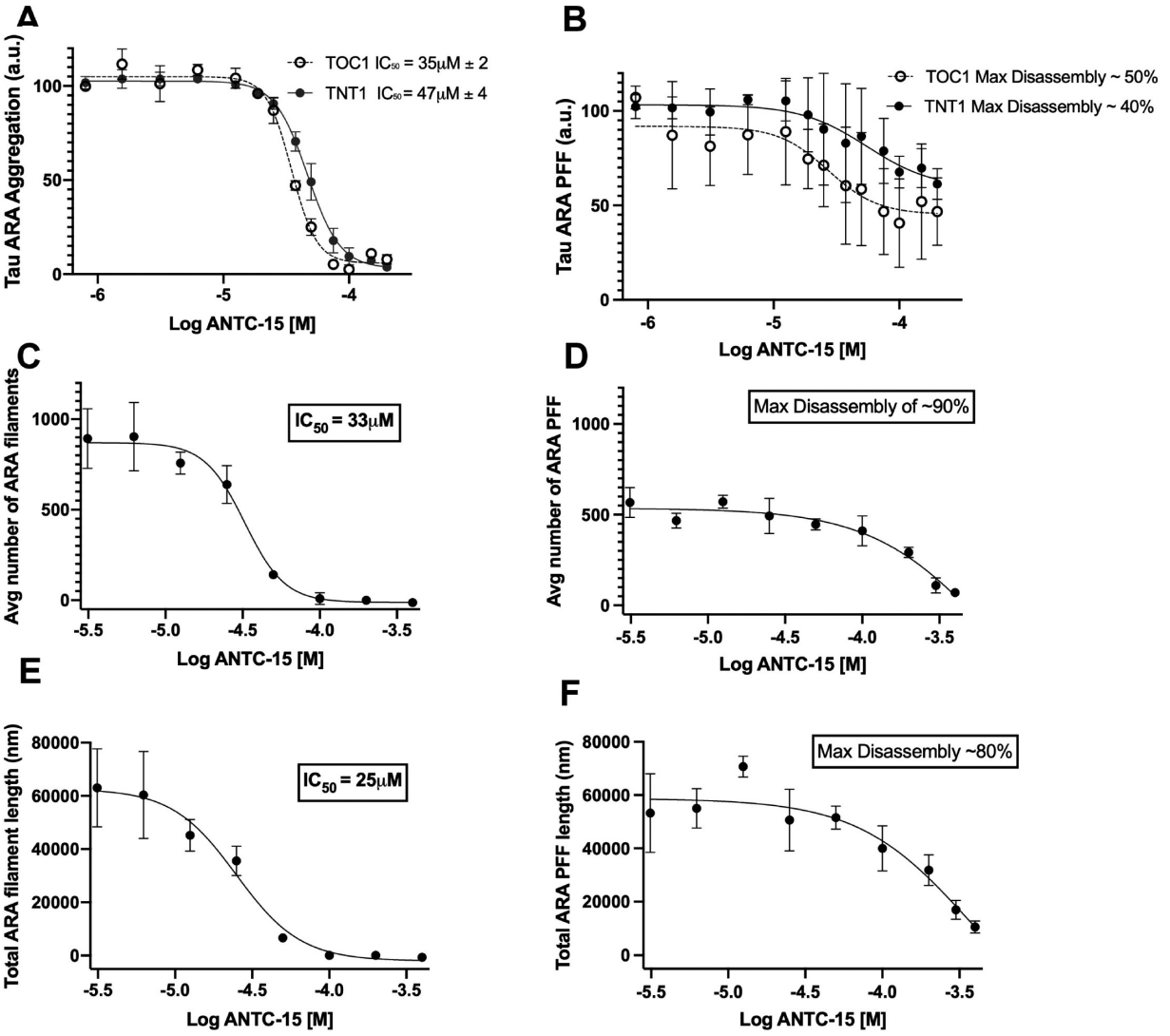

Figure 5. ANTC-15 dose dependence: (A, C, and E) inhibition of ARA filaments and (B, D, and F) disassembly of ARA preformed filaments (PFF). Inhibition and disassembly of both TOC1 (○) and TNT (●) reactive species as shown by a sandwich ELISA at different concentrations of ANTC-15 (A and B). Inhibition and disassembly of the average number of filaments as determined by TEM at different concentrations of ANTC-15 (C and D). Inhibition and disassembly of total filament length as determined by TEM at different concentrations of ANTC-15 (E and F).

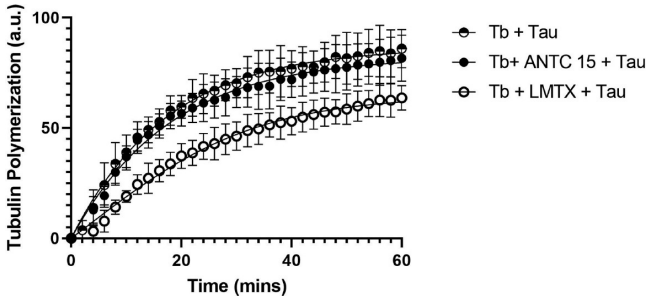

Figure 6. Tubulin polymerization assay. Tubulin (Tb) at a final concentration of 2 mg/mL was incubated at 37 °C with or without an inhibitor compound at a concentration of 40 μM in the presence of 0.5 μM tau. Data were then normalized against a Taxol (10 μM) positive control and fit to a Finke−Watzky polymerization curve.

develop compounds that can not only inhibit filament formation but also disassemble previously formed filaments. Due to the thermodynamic stability of the amyloid fold formed during tau aggregation, filaments are extremely stable. This stability means using inhibitory molecules to prevent the conversion of inert monomeric tau to aggregate competent monomer, or aggregated tau, is not sufficient to disassemble previously formed filaments. Unfortunately, current compound screening approaches have not yet provided a viable therapeutic that has been successful in phase III clinical trials. The phenothiazine tau aggregation inhibitor compound LMTX showed some promise in early clinical studies but did not meet pretrial objectives in comparison with the placebo control of a small LMTX dose.[8] Further trials with small doses of LMTX are currently underway.[27]

Our efforts to identify TAIs from the fungal secondary metabolome of *A. nidulans* have yielded several compounds with TAI activity,[18,19] including the isoquinoline compound ANTC-15 identified in this study. ANTC-15 almost completely inhibited the formation of ARA-induced filaments at a compound concentration of 100 μM as shown by an oligomer-specific antibody ELISA and EM. ANTC-15 also disassembled ARA preformed filaments at high compound concentrations by almost 50% as determined by an ELISA and

https://doi.org/10.1021/acs.biochem.1c00111
Biochemistry 2021, 60, 1658−1669

80−90% as determined by EM. We interpret this difference as potentially being due to differences in the sensitivity of the assays. For example, the capture antibodies used in the sandwich ELISA are conformationally sensitive antibodies with a high affinity for aggregated tau protein. The protocol was carefully optimized by titering the antibodies against a standard curve of diluted aggregate and monomeric samples to ensure that the differentiation between monomeric and aggregated tau in our reactions was in a linear range (Figure S2). However, it is likely that TOC1 and TNT1 antibodies bind to structures smaller than the approximately 25 nm limit of resolution of TEM.

Using dose dependence studies of ANTC-15 to inhibit ARA-induced fibrils, we were able to calculate the IC_{50} of ANTC-15 being between 25 and 47 μM, depending on the assay used, ELISA or TEM (Figure 5A,C,E). The inhibition dose−response curves show high Hill coefficients (>1.5) as summarized in Table S3. Hill coefficient values of >1 are typically considered to be an indication of a complex inhibitory mechanism. Many previously identified tau aggregation inhibitors have also been reported to have Hill coefficients of >1 as shown by the NIH databank entry AID 1460. As discussed by Prinz,[37] there could be several reasons for a Hill coefficient not being equal to 1, including ligand cooperativity or ligand micellization, a protein:ligand stoichiometry not equal to 1:1, protein denaturation that leads to an increase in the number of ligand binding sites, or a complex mixture of several of these factors.

Due to the hydrophobic nature of ANTC-15, it is unlikely to be a biologically useful compound in its current form. In addition, potential hydrophobic interactions between ANTC-15 and the ARA inducer molecule cannot be ignored. However, the ability of ANTC-15 to disassemble the extremely stable ARA PFF suggests that its activity is not solely due to interactions with the ARA inducer.

Although ANTC-15 has activity to inhibit tau aggregation and disassemble preformed filaments, the micromolar concentration required for this activity is too high for it to be considered a potential therapeutic candidate as most drugs tend to be effective at nanomolar concentrations. However, we were interested to see if ANTC-15 could be used as a molecular probe for further investigation of *in vitro* tau aggregation models. We therefore used the TAI LMTX as an external benchmark that had already been shown to inhibit tau filament formation at relatively low concentrations in both *in vitro* and *in vivo* assays. To our surprise, LMTX had very little effect on the formation of ARA filaments or in disassembling ARA preformed filaments both in ELISAs and as determined by EM.

Because LMTX was first identified as a TAI using heparin as an inducer of tau aggregation rather than ARA,[9] we sought to test both ANTC-15 and LMTX against heparin-induced filaments. The results were opposite to those obtained with ARA-induced filaments. LMTX was effective as a TAI against heparin-induced filament formation, while ANTC-15 had little to no TAI activity against heparin-induced aggregation. The most striking example of this is that at 200 μM LMTX, the very long filaments characteristic of heparin-induced aggregation were virtually nonexistent. In the presence of ANTC-15, there was little to no reduction in the number of long heparin-induced filaments (although there was an increase in the number of smaller filaments). ANTC-15 also had no effect on heparin preformed filaments, while the addition of LMTX to heparin preformed filaments actually increased the number of TOC1 reactive species and had no significant effect on TNT1 reactive species, though an increase in the number of smaller filaments was observed by EM. This increase in the number of smaller filaments could account for the increase in the level of TOC1 reactive species as breaking down filaments can result in increased antibody binding site availability. For example, acoustic shearing can be used to break apart long filaments into small oligomers and therefore increase the number of available binding sites of both TOC1 and TNT1 antibodies (Figure S8). Although tau aggregation in disease is still not fully understood, it is widely accepted that small oligomers may play an important role in pathology.[38−40] Therefore, potential therapeutic candidates that inhibit tau filament formation but promote the formation of smaller oligomers may potentially increase the neurodegenerative effects of tau aggregation. There is also a growing consensus that the spread of tau aggregation occurs in a prion-like fashion, where inert monomeric tau is converted to a seed-competent tau aggregate that can further oligomerize.[41] For these reasons, it is important to study the effects of TAIs on the formation of large filaments and oligomers using visualization methods such as TEM as well as conformational changes to the protein using immunohistochemical techniques.

Recent developments in cryo-electron microscopy have allowed researchers to determine high-resolution structures of tau fibrils isolated from multiple tauopathies.[11−13] These discoveries have shed new light on, and garnered support for, the hypothesis that tau fibrils from different diseases are distinct structures with unique properties. In light of this finding, it is important that we identify inducers that form disease relevant filaments *in vitro* to screen potential therapeutic TAI compounds. *In vitro* models will likely have to be disease-specific. For example, a potent compound that targets the interface between PHFs in AD is unlikely to be as effective against the different set of residues at the interface of filaments from Pick's disease. In addition, cryo-EM and pulsed electron paramagnetic resonance structural studies have revealed that at least one common *in vitro* aggregation inducer (heparin) does not appear to form structures relevant to disease.[16,42] These findings may explain why potential therapeutic molecules that inhibit filaments *in vitro* and in specific *in vivo* models have poor results when used in humans in clinical trials.[43] In this study, we have shown how two different small molecules can have quite different effects on assembly and disassembly of filaments induced by ARA versus those induced by heparin.

Molecular dynamics and drug discovery efforts using heparin-induced tau filaments may not represent the true nature of authentic tau aggregation *in vivo*. While a compelling argument can be made for arachidonic acid as a biologically relevant aggregation inducer of tau due to (1) its relative abundance in the cell, especially during times of oxidative stress, (2) *in vitro* filaments appearing to have gross morphological traits similar to those of the straight filaments isolated from AD with regard to average length, width, and periodicity,[23] and (3) antibodies that have been raised against ARA-induced filaments having a high affinity for epitopes in diseased AD brain tissue, as well as tissue isolated from CTE brains,[28,31] to date there are no high-resolution structures of arachidonic acid-induced filaments, and therefore, the atomic similarities to filaments from diseases are unknown.

https://doi.org/10.1021/acs.biochem.1c00111
Biochemistry 2021, 60, 1658−1669

Our data are consistent with the possibility that ARA and heparin induce the formation of tau aggregates that are structurally distinct and that ANTC15 and LMTX have differing activities against the two structures. Because of the differences in the properties of the inducers and because of differences in the chemical structures of the compounds, we cannot rule out the possibility that our results could be explained by a more complex mechanism beyond any potential structural differences in ARA and heparin filaments. For example, ANTC-15 is highly hydrophobic and could have a preferential interaction with ARA or ARA/tau complexes. Similarly, LMTX could have a preferential interaction with the polyanionic heparin inducer. These and potentially other complexities could help to explain the very steep dose−response curves of inhibition observed. Further experimentation will be required to fully elucidate the mechanisms of inhibition and disassembly. However, unless future structural studies can demonstrate that these *in vitro* filaments have structures related to those found in disease, the mechanisms of inhibition may not be directly biologically relevant to AD and ADRDs.

Our data suggest that it is important to begin developing new screening techniques that utilize a range of different types of tau aggregation inducer molecules, seeding assays, and spontaneous aggregation models, rather than relying on one particular inducer molecule. Long-term goals must be to identify whether artificially induced aggregates *in vitro* generate structures relevant to disease and to identify to which disease they are specific, to enhance the potential for success in future clinical trials. Until we can verify that artificially induced *in vitro* tau aggregates have sufficient structural similarities to those found in disease, the evaluation of potential TAIs such as ANTC-15 must be interpreted with an abundance of caution.

■ ASSOCIATED CONTENT

Supporting Information

The Supporting Information is available free of charge at https://pubs.acs.org/doi/10.1021/acs.biochem.1c00111.

Figures S1−S8, the synthesis of ANTC-15, and Tables S1−S3 (PDF)

Accession Codes

MAPT, P10636.

■ AUTHOR INFORMATION

Corresponding Authors

David J. Ingham − *Department of Molecular Biosciences, University of Kansas, Lawrence, Kansas 66045, United States*; Email: inghamd002@ku.edu

Truman Christopher Gamblin − *Department of Molecular Biosciences, University of Kansas, Lawrence, Kansas 66045, United States; Department of Biology, The University of Texas at San Antonio, San Antonio, Texas 78249, United States*; orcid.org/0000-0001-7498-1524; Email: truman.gamblin@UTSA.edu

Authors

Bryce R. Blankenfeld − *Department of Molecular Biosciences, University of Kansas, Lawrence, Kansas 66045, United States*

Shibin Chacko − *Synthetic Chemical Biology Core Facility, University of Kansas, Lawrence, Kansas 66047, United States*

Chamani Perera − *Synthetic Chemical Biology Core Facility, University of Kansas, Lawrence, Kansas 66047, United States*

Berl R. Oakley − *Department of Molecular Biosciences, University of Kansas, Lawrence, Kansas 66045, United States*; orcid.org/0000-0002-3046-8240

Complete contact information is available at: https://pubs.acs.org/10.1021/acs.biochem.1c00111

Author Contributions

D.J.I. completed inhibition and disassembly studies and drafted the manuscript. B.R.B. completed the initial inhibitory and disassembly assays of ANTC-15 as a TAI. C.P. completed synthesis of ANTC-15. B.R.O. and T.C.G. conceived the original studies, participated in their design and coordination, and helped draft the manuscript. All authors have read and approved the final manuscript.

Funding

National Institute of General Medical Sciences of the National Institutes of Health (Grants P20GM113117 and P20GM103638 to S.C. and C.P.), National Institute on Aging of the National Institutes of Health (Grant R21 AG069112 to T.C.G.), Roofe Fellowship, KU Endowment, and the Institute for Neurological Discoveries (D.J.I.), and the National Institute of General Medical Sciences Graduate Training Program in Dynamic Aspects of Chemical Biology (Grant T32 GM008545 to D.J.I. and B.R.B.). Initial compound discovery work was supported by the H. L. Snyder Medical Foundation (B.R.O. and T.C.G.).

Notes

The authors declare no competing financial interest.

■ ACKNOWLEDGMENTS

The authors thank Kelsey Hillyer for help in quantifying TEM images, Maritza Quintero (The University of Texas at San Antonio) for providing comments and suggestions about the manuscript, and Dr. Nicholas Kanaan (Michigan State University) for his kind gift of TOC and TNT antibodies.

■ ABBREVIATIONS

TAI, tau aggregation inhibitor; ARA, arachidonic acid; HEP, heparin; AD, Alzheimer's disease; CTE, chronic traumatic encephalopathy; MAPT, microtubule-associated protein tau; LMTM/LMTX/TauRx0237, leucomethylthionium; PFF, preformed fibrils; ThS, thioflavin S; TEM, transmission electron microscopy; ELISA, enzyme-linked immunosorbent assay.

■ REFERENCES

(1) 2020 Alzheimer's disease facts and figures (2020) *Alzheimer's Dementia 16* (3), 391−460.

(2) La Joie, R., Visani, A. V., Baker, S. L., Brown, J. A., Bourakova, V., Cha, J., Chaudhary, K., Edwards, L., Iaccarino, L., Janabi, M., Lesman-Segev, O. H., Miller, Z. A., Perry, D. C., O'Neil, J. P., Pham, J., Rojas, J. C., Rosen, H. J., Seeley, W. W., Tsai, R. M., Miller, B. L., Jagust, W. J., and Rabinovici, G. D. (2020) Prospective longitudinal atrophy in Alzheimer's disease correlates with the intensity and topography of baseline tau-PET. *Sci. Transl. Med. 12* (524), eaau5732.

(3) Wang, Y., and Mandelkow, E. (2016) Tau in physiology and pathology. *Nat. Rev. Neurosci. 17* (1), 22−35.

(4) Cummings, J. L., Tong, G., and Ballard, C. (2019) Treatment Combinations for Alzheimer's Disease: Current and Future Pharmacotherapy Options. *J. Alzheimer's Dis. 67* (3), 779−794.

(5) Bulic, B., Pickhardt, M., and Mandelkow, E. (2013) Progress and Developments in Tau Aggregation Inhibitors for Alzheimer Disease. *J. Med. Chem. 56* (11), 4135−4155.

(6) Pickhardt, M., Larbig, G., Khlistunova, I., Coksezen, A., Meyer, B., Mandelkow, E.-M., Schmidt, B., and Mandelkow, E. (2007) Phenylthiazolyl-hydrazide and its derivatives are potent inhibitors of tau aggregation and toxicity in vitro and in cells. *Biochemistry 46* (35), 10016.
(7) Chang, E., Honson, N. S., Bandyopadhyay, B., Funk, K. E., Jensen, J. R., Kim, S., Naphade, S., and Kuret, J. (2009) Modulation and detection of tau aggregation with small-molecule ligands. *Curr. Alzheimer Res. 6* (5), 409−414.
(8) Gauthier, S., Feldman, H. H., Schneider, L. S., Wilcock, G. K., Frisoni, G. B., Hardlund, J. H., Moebius, H. J., Bentham, P., Kook, K. A., Wischik, D. J., Schelter, B. O., Davis, C. S., Staff, R. T., Bracoud, L., Shamsi, K., Storey, J. M. D., Harrington, C. R., and Wischik, C. M. (2016) Efficacy and safety of tau-aggregation inhibitor therapy in patients with mild or moderate Alzheimer's disease: a randomised, controlled, double-blind, parallel-arm, phase 3 trial. *Lancet 388* (10062), 2873−2884.
(9) Taniguchi, S., Suzuki, N., Masuda, M., Hisanaga, S.-I., Iwatsubo, T., Goedert, M., and Hasegawa, M. (2005) Inhibition of heparin-induced tau filament formation by phenothiazines, polyphenols, and porphyrins. *J. Biol. Chem. 280* (9), 7614−7623.
(10) Sanders, D. W., Kaufman, S. K., DeVos, S. L., Sharma, A. M., Mirbaha, H., Li, A., Barker, S. J., Foley, A. C., Thorpe, J. R., Serpell, L. C., Miller, T. M., Grinberg, L. T., Seeley, W. W., and Diamond, M. I. (2014) Distinct tau prion strains propagate in cells and mice and define different tauopathies. *Neuron 82* (6), 1271−1288.
(11) Falcon, B., Zivanov, J., Zhang, W., Murzin, A. G., Garringer, H. J., Vidal, R., Crowther, R. A., Newell, K. L., Ghetti, B., Goedert, M., and Scheres, S. H. W. (2019) Novel tau filament fold in chronic traumatic encephalopathy encloses hydrophobic molecules. *Nature 568* (7752), 420−423.
(12) Goedert, M., Falcon, B., Zhang, W., Ghetti, B., and Scheres, S. H. W. (2018) Distinct Conformers of Assembled Tau in Alzheimer's and Pick's Diseases. *Cold Spring Harbor Symp. Quant. Biol. 83*, 163−171.
(13) Zhang, W., Tarutani, A., Newell, K. L., Murzin, A. G., Matsubara, T., Falcon, B., Vidal, R., Garringer, H. J., Shi, Y., Ikeuchi, T., Murayama, S., Ghetti, B., Hasegawa, M., Goedert, M., and Scheres, S. H. W. (2020) Novel tau filament fold in corticobasal degeneration. *Nature 580*, 283−287.
(14) Falcon, B., Zhang, W., Schweighauser, M., Murzin, A. G., Vidal, R., Garringer, H. J., Ghetti, B., Scheres, S. H. W., and Goedert, M. (2018) Tau filaments from multiple cases of sporadic and inherited Alzheimer's disease adopt a common fold. *Acta Neuropathol. 136* (5), 699−708.
(15) Fichou, Y., and Han, S. (2019) Protein shapes at the core of chronic traumatic encephalopathy. *Nat. Struct. Mol. Biol. 26* (5), 336−338.
(16) Zhang, W., Falcon, B., Murzin, A. G., Fan, J., Crowther, R. A., Goedert, M., and Scheres, S. H. (2019) Heparin-induced tau filaments are polymorphic and differ from those in Alzheimer's and Pick's diseases. *eLife 8*, e43584.
(17) Carlson, S. W., Branden, M., Voss, K., Sun, Q., Rankin, C. A., and Gamblin, T. C. (2007) A Complex Mechanism for Inducer Mediated Tau Polymerization. *Biochemistry 46* (30), 8838−8849.
(18) Paranjape, S. R., Chiang, Y. M., Sanchez, J. F., Entwistle, R., Wang, C. C., Oakley, B. R., and Gamblin, T. C. (2014) Inhibition of Tau Aggregation by Three Aspergillus nidulans Secondary Metabolites: 2,omega-Dihydroxyemodin, Asperthecin, and Asperbenzaldehyde. *Planta Med. 80* (1), 77−85.
(19) Paranjape, S. R., Riley, A. P., Somoza, A. D., Oakley, C. E., Wang, C. C., Prisinzano, T. E., Oakley, B. R., and Gamblin, T. C. (2015) Azaphilones inhibit tau aggregation and dissolve tau aggregates in vitro. *ACS Chem. Neurosci. 6* (5), 751−760.
(20) Ahuja, M., Chiang, Y. M., Chang, S. L., Praseuth, M. B., Entwistle, R., Sanchez, J. F., Lo, H. C., Yeh, H. H., Oakley, B. R., and Wang, C. C. (2012) Illuminating the diversity of aromatic polyketide synthases in Aspergillus nidulans. *J. Am. Chem. Soc. 134* (19), 8212−8221.
(21) Grandjean, J.-M. M., Jiu, A. Y., West, J. W., Aoyagi, A., Droege, D. G., Elepano, M., Hirasawa, M., Hirouchi, M., Murakami, R., Lee, J., Sasaki, K., Hirano, S., Ohyama, T., Tang, B. C., Vaz, R. J., Inoue, M., Olson, S. H., Prusiner, S. B., Conrad, J., and Paras, N. A. (2020) Discovery of 4-Piperazine Isoquinoline Derivatives as Potent and Brain-Permeable Tau Prion Inhibitors with CDK8 Activity. *ACS Med. Chem. Lett. 11* (2), 127−132.
(22) Rankin, C. A., Sun, Q., and Gamblin, T. C. (2005) Pseudo-phosphorylation of tau at Ser202 and Thr205 affects tau filament formation. *Mol. Brain Res. 138* (1), 84−93.
(23) King, M. E., Gamblin, T. C., Kuret, J., and Binder, L. I. (2000) Differential Assembly of Human Tau Isoforms in the Presence of Arachidonic Acid. *J. Neurochem. 74* (4), 1749−1757.
(24) Combs, B., Tiernan, C. T., Hamel, C., and Kanaan, N. M. (2017) Production of recombinant tau oligomers in vitro. *Methods Cell Biol. 141*, 45−64.
(25) Combs, B., Voss, K., and Gamblin, T. C. (2011) Pseudohyperphosphorylation Has Differential Effects on Polymerization and Function of Tau Isoforms. *Biochemistry 50* (44), 9446−9456.
(26) Mutreja, Y., and Gamblin, T. C. (2017) Methods in Tau Cell Biology Optimization of in vitro conditions to study the arachidonic acid induction of 4R isoforms of the microtubule-associated protein tau. *Methods Cell Biol. 141*, 65−88.
(27) Wilcock, G. K., Gauthier, S., Frisoni, G. B., Jia, J., Hardlund, J. H., Moebius, H. J., Bentham, P., Kook, K. A., Schelter, B. O., Wischik, D. J., Davis, C. S., Staff, R. T., Vuksanovic, V., Ahearn, T., Bracoud, L., Shamsi, K., Marek, K., Seibyl, J., Riedel, G., Storey, J. M. D., Harrington, C. R., and Wischik, C. M. (2017) Potential of Low Dose Leuco-Methylthioninium Bis(Hydromethanesulphonate) (LMTM) Monotherapy for Treatment of Mild Alzheimer's Disease: Cohort Analysis as Modified Primary Outcome in a Phase III Clinical Trial. *J. Alzheimer's Dis. 61* (1), 435−457.
(28) Ward, S. M., Himmelstein, D. S., Ren, Y., Fu, Y., Yu, X. W., Roberts, K., Binder, L. I., and Sahara, N. (2014) TOC1: a valuable tool in assessing disease progression in the rTg4510 mouse model of tauopathy. *Neurobiol. Dis. 67*, 37−48.
(29) Kanaan, N. M., Cox, K., Alvarez, V. E., Stein, T. D., Poncil, S., and McKee, A. C. (2016) Characterization of Early Pathological Tau Conformations and Phosphorylation in Chronic Traumatic Encephalopathy. *J. Neuropathol. Exp. Neurol. 75* (1), 19−34.
(30) Mufson, E. J., Ward, S., and Binder, L. (2014) Prefibrillar tau oligomers in mild cognitive impairment and Alzheimer's disease. *Neurodegener. Dis. 13* (2−3), 151−153.
(31) Combs, B., Hamel, C., and Kanaan, N. M. (2016) Pathological conformations involving the amino terminus of tau occur early in Alzheimer's disease and are differentially detected by monoclonal antibodies. *Neurobiol. Dis. 94*, 18−31.
(32) Arendt, T., Stieler, J. T., and Holzer, M. (2016) Tau and tauopathies. *Brain Res. Bull. 126* (Part 3), 238−292.
(33) Soeda, Y., Saito, M., Maeda, S., Ishida, K., Nakamura, A., Kojima, S., and Takashima, A. (2019) Methylene Blue Inhibits Formation of Tau Fibrils but not of Granular Tau Oligomers: A Plausible Key to Understanding Failure of a Clinical Trial for Alzheimer's Disease. *J. Alzheimer's Dis. 68* (4), 1677−1686.
(34) Harrington, C. R., Storey, J. M. D., Clunas, S., Harrington, K. A., Horsley, D., Ishaq, A., Kemp, S. J., Larch, C. P., Marshall, C., Nicoll, S. L., Rickard, J. E., Simpson, M., Sinclair, J. P., Storey, L. J., and Wischik, C. M. (2015) Cellular Models of Aggregation-dependent Template-directed Proteolysis to Characterize Tau Aggregation Inhibitors for Treatment of Alzheimer Disease. *J. Biol. Chem. 290* (17), 10862.
(35) Götz, J., Ittner, A., and Ittner, L. M. (2012) *Tau-targeted treatment strategies in Alzheimer's disease*, Vol. *165*, pp 1246−1259, Oxford University Press, Oxford, U.K.
(36) Spillantini, M. G., and Goedert, M. (2013) Tau pathology and neurodegeneration. *Lancet Neurol. 12* (6), 609−622.
(37) Prinz, H. (2010) Hill coefficients, dose-response curves and allosteric mechanisms. *Journal of chemical biology 3* (1), 37−44.

https://doi.org/10.1021/acs.biochem.1c00111
Biochemistry 2021, 60, 1658−1669

(38) Tiernan, C. T., Mufson, E. J., Kanaan, N. M., and Counts, S. E. (2018) Tau Oligomer Pathology in Nucleus Basalis Neurons During the Progression of Alzheimer Disease. *J. Neuropathol. Exp. Neurol. 77* (3), 246−259.
(39) Castillo-Carranza, D. L., Gerson, J. E., Sengupta, U., Guerrero-Munoz, M. J., Lasagna-Reeves, C. A., and Kayed, R. (2014) Specific targeting of tau oligomers in Htau mice prevents cognitive impairment and tau toxicity following injection with brain-derived tau oligomeric seeds. *J. Alzheimer's Dis. 40* (Suppl. 1), S97−S111.
(40) Shafiei, S. S., Guerrero-Muñoz, M. J., and Castillo-Carranza, D. L. (2017) Tau Oligomers: Cytotoxicity, Propagation, and Mitochondrial Damage. *Front. Aging Neurosci. 9*, 83.
(41) Mirbaha, H., Chen, D., Morazova, O. A., Ruff, K. M., Sharma, A. M., Liu, X., Goodarzi, M., Pappu, R. V., Colby, D. W., Mirzaei, H., Joachimiak, L. A., and Diamond, M. I. (2018) Inert and seed-competent tau monomers suggest structural origins of aggregation. *eLife 7*, e36584.
(42) Fichou, Y., Vigers, M., Goring, A. K., Eschmann, N. A., and Han, S. (2018) Heparin-induced tau filaments are structurally heterogeneous and differ from Alzheimer's disease filaments. *Chem. Commun. (Cambridge, U. K.) 54* (36), 4573−4576.
(43) Cummings, J. L., Morstorf, T., and Zhong, K. (2014) Alzheimer's disease drug-development pipeline: few candidates, frequent failures. *Alzheimer's Res. Ther. 6* (4), 37.

https://doi.org/10.1021/acs.biochem.1c00111
Biochemistry 2021, 60, 1658−1669